

# Chapter 3

## Effect on the Microstructure and Mechanical Properties of the Structural Steel Welded in Marine Environment

M. Flores, J.J. Ruiz, F. Macías, and J. Acevedo

**Abstract** Recently, oil deposits were found in ever deeper waters. In this context, it is important to study the water depth effect on parameters in repair and maintenance operations of pipelines for extraction and/or transportation of crude oil, of which there is limited information in literature. This paper shows a study of the effect of the water depth on the microstructure and mechanical properties in joining structural steel welded in a marine environment in steels with a maximum CE (carbon equivalent) of 0.37 %. Wet welding coupons of steel ASTM A36 were joined by the manual metal arc welding (MMAW) process at depths of 10, 20, 30, and 40 m, using AWS Broco SoftTouch as filler metal (3.17 mm diameter) inside a simulation hyperbaric chamber. Image analysis was applied to welded coupons, with the aim to obtain the phase quantification and porosity as well as mechanical properties. The results show that there is an inverse relationship between the increase in depth at which the welding is performed and the mechanical properties, while the filler metal properties were kept constant. Microstructural changes vary as a function of the depth at which repair-maintenance is performed, with an increase in growing phase shift which is highly undesirable because of their brittleness and hardness.

**Keywords** MMAW • Wet • Welding • Mechanical properties • Depth

### 3.1 Introduction

The success in looking for light oil in deep water and the growth of the offshore energy industry and the need to build submerged such as offshore platforms and pipelines themselves of this economic activity driving, make wet welding becomes one of the most efficient options for the construction, repair, and maintenance of offshore structure site options, due to the low cost and the time of application [1]. Currently, the marine environment solder is applied in two main ways: the first is the

---

M. Flores (✉) • J.J. Ruiz • F. Macías • J. Acevedo.  
COMIMSA-Salttillo, Calle Ciencia y Tecnología # 790, C.P: 25290 Saltillo, Coah., Mexico  
e-mail: [mflores@comimsa.com](mailto:mflores@comimsa.com)

underwater welding in a wet environment, which is done directly in the submerged part, and the second is the underwater welding in a dry environment, which allows the diver/welder be within a habitat that provides a dry environment under a body of water [2].

It has been shown to influence the depth variation along multipass wet underwater welding and the mechanical properties of steels, using stress tests observing the decrease in the tensile strength with increasing depth. This relationship is promoted with increasing of depth and porosity [3].

Johnson et al. [4] show that the wet marine welding of steels produces three basic microstructures: ferrite, bainite, and martensite. This author also discusses the environmental effects of water, such as salinity and pressure change, on the chemistry and microstructure of the welded metal, but just mentions that the effect of water temperature in the cooling rate is small. On the other hand, Hernandez [5] demonstrated that due to rapid cooling and solidification of the weld metal, ferrite and allotriomorphic ferrite are formed. Also, Hernández and Ballesteros [5, 6] comment that the depth is not an important factor affecting the microstructure for the 10–40 m of depth. Currently, wet welding has become one of the most efficient options for the construction, repair, and in-site maintenance of offshore structures due to the low cost and the application time.

So, one of the main problems of wet welding is the decomposition of water (hydrogen and oxygen) that interacts strongly with the weld pool; this causes the formation of pores, cracks, and nonmetallic inclusions that affect the mechanical properties of the cord. Also, cooling is subjected to the welding that affects the mechanical properties of the cord provoking the appearance of a microstructure susceptible to cracking hydrogen and also contributing to the rapid gas retention during solidification of the weld metal [7, 8].

The work performed previously does not clarify the effect of depth in the microstructure and mechanical properties. For this reason, in this work presents result in the pressure range 10–40 m deep in structural steels used in offshore, in order to contribute to the development of welded joints working at different depths.

## 3.2 Experimental

An experiment was conducted at different depths of 10, 20, 30, and 40 m using ASTM A36 steel like base material, which is used for building structures in the coast, structures in offshore platforms, piers piles, pipes driving, piles of bridges, ships, etc. [9]. The chemical composition of ASTM A36 steel plate is shown in Table 3.1 [10]. This steel presents a tensile strength of 58,000–80,000 PSI and yield stress of 36,000 PSI [10]. The steel has a carbon equivalent of 0.3 suggesting that have good weldability under water and are not susceptible to hydrogen cracking, so the ASTM A36 structural steel with  $CE = 0.3093$  meets this requirement [11].

**Table 3.1** Chemical composition according to the results of chemical analysis to ASTM A36 steel plate, % e.p.) (% parts per million)

ASTM A36	Fe	C	Mn	Si	Cr	Ni	P
	98.77	0.16	0.83	0.11	0.02	0.04	0.013
	S	Mo	Cu	V	Nb	Ti	W
	0.004	0.01	0.022	0.004	0.007	0.004	0.002

**Fig. 3.1** Design of the joint bevel in “V” with support for the realization of the test welds in steel ASTM A36

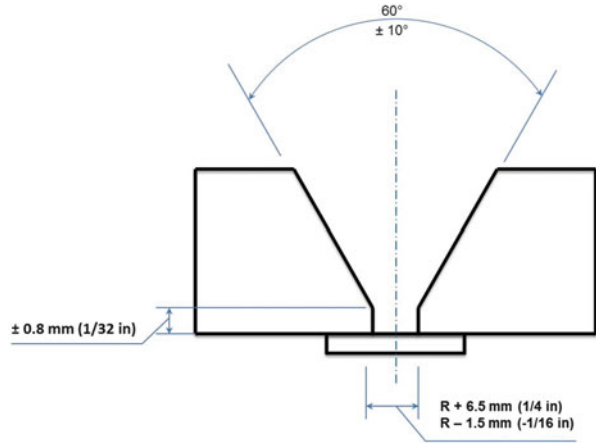


**Table 3.2** Chemical composition of coated electrode Broco Underwater Soft-Touch E7014 [10]

Designation (% e.p.)								
AWS E7014	C	Si	Mn	P	S	Cu	Al	Cr
	0.072	0.244	1.185	0.012	0.002	0.016	0.024	0.024
	Mo	Ni	V	Ti	Nb	Co	Fe	
	0.005	0.023	0.015	0.008	0.017	0.009	Bal.	

E70XX electrodes like filler metal were used during the MMAW process, the experiment was conducted in a hyperbaric chamber pressurized with capacity of 31 atm (atmosphere) absolute pressure equal to 300m depth. The welding system has a multi-process machine 300 A with direct current and constant voltage up to 29 V, with an efficiency of 100 %. Samples were prepared for metallography and tensile tests [10].

The joints were prepared with bevel “V” with support for the application of wet welding cords as shown in Fig. 3.1.

Table 3.2 shows the chemical composition of the coated electrode Broco Underwater SoftTouch E7014 used as filler for performing wet stamps. This electrode has a tensile strength of 70,000 PSI [10].

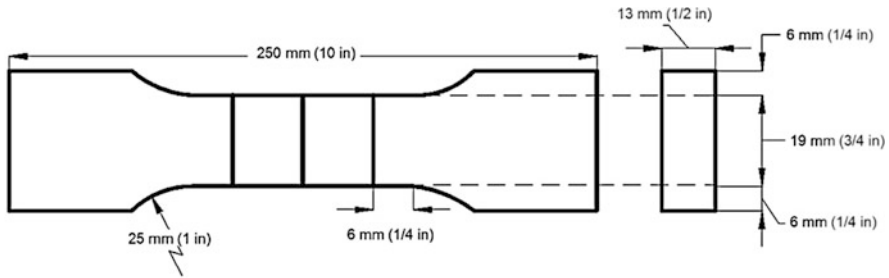


Fig. 3.2 Schematic representation of tensile specimen dimensions [11]

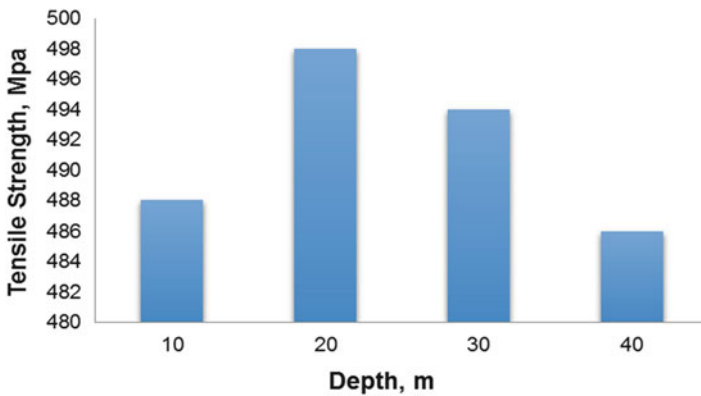
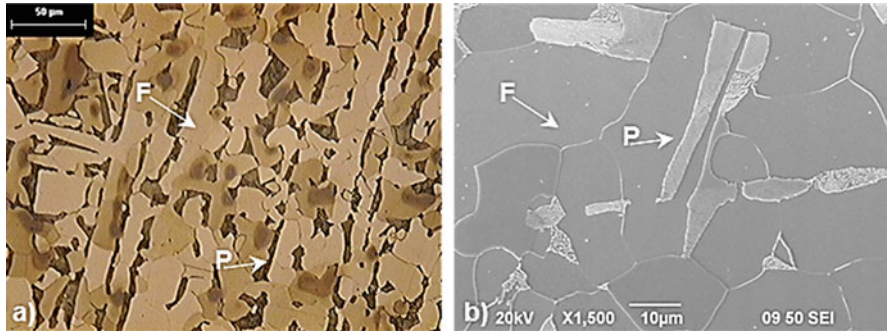


Fig. 3.3 Results of tensile tests in function of welding deep

For metallographic microstructure analysis,  $\text{HNO}_3$  5 % (Nital) was used for 10 s for a subsequent observation of the microstructure obtained through an Olympus PMG-3, and Klemm's y was used for 30 s. Phase quantification was performed using the software AxioVision Rel. 4.8. Tensile tests were performed with a Tinius Olsen Super L290 machine with a load of 600 kN; samples were machined according to AWS D3.6 [11]. In Fig. 3.2, dimensions of the specimen are shown.

### 3.3 Results and Discussion

Figure 3.3 shows the results of tensile tests on samples developed at different depths are exhibited. It is observed that at 10 m, the tensile strength is 488 MPa, while at 20 m it increases to 498 MPa; this value decreases slightly at depths of 30 m with 494 MPa and 40 m with 486 MPa. The results confirm that with increasing depth, the tensile strength tends to decrease, with a notable increase in tension at 20 m.



**Fig. 3.4** A36 steel micrographs obtained in (a) optical microscope at 50 $\times$  attacked with Klemm's and in (b) SEM at 1500 $\times$  attacked with Nital 5%, where F=ferrite and (P)=pearlite

Figure 3.4 shows micrographs taken in the base metal, A36, in (a) optical microscope at 50 $\times$  and (b) SEM (scanning electron microscope) to 1500 $\times$ , where a ferrite-pearlite matrix is observed with an average hardness of 157 HV.

Figure 3.5 shows micrographs taken at 50 $\times$  of each of the depths studied, in the HAZ (heat-affected zone), and weld metal (MA) is shown. It is seen in the HAZ at depths of 10 m which is constituted by Widmanstätten ferrite (FW), martensite block (M), ferrite in the grain boundary (FLG), and ferrite blocks, while the filler metal matrix mostly found acicular ferrite, ferrite blocks, and FLG. The same microstructures are presented in the other in different depth percentages; also observed in the specimen of 40 m is the presence of microcracks in the HAZ, where the phases were Widmanstätten ferrite and martensite blocks.

The results of the quantification phases are shown in Figs. 3.6 and 3.7. In Fig. 3.6, the variation of the percentage of phase with respect to the depth is shown. The phases present in the filler metal weld bead have a higher percentage of ferrite in block and acicular ferrite, without the presence of martensite and bainite. The ferrite in block is one of the phases having a greater variation as a function of the depth of welding at 10 m depth is 75% and increases to 95% at 30 m. While at 20 m depth, the microstructure has 73% of ferrite block (acicular ferrite) and only 3% Widmanstätten ferrite. At 20 m depth the content of acicular ferrite is bigger and lower content of FLG Widmanstätten ferrite was observed.

Figure 3.7 shows the microstructure present in the HAZ, which shows that there is a Widmanstätten ferrite increase with increasing depth. At 10 m, FW content is 40–65% increasing to 40 m, and the content of acicular ferrite remains in the specimen of 20 m and 40 m with an average of 9%.

Both block martensite and bainite are present in the samples welded at 10, 30, and 40 m finding a maximum of 1.8% to note that these phases were found mainly in areas between steps. The content of the ferrite block is held constant at depths of 10, 20, and 30 m at 50% and decreases to 40–26% m, while the FLG at 20 m has the highest content up to 6%, and this is decreasing to less than 1% at 40 m.

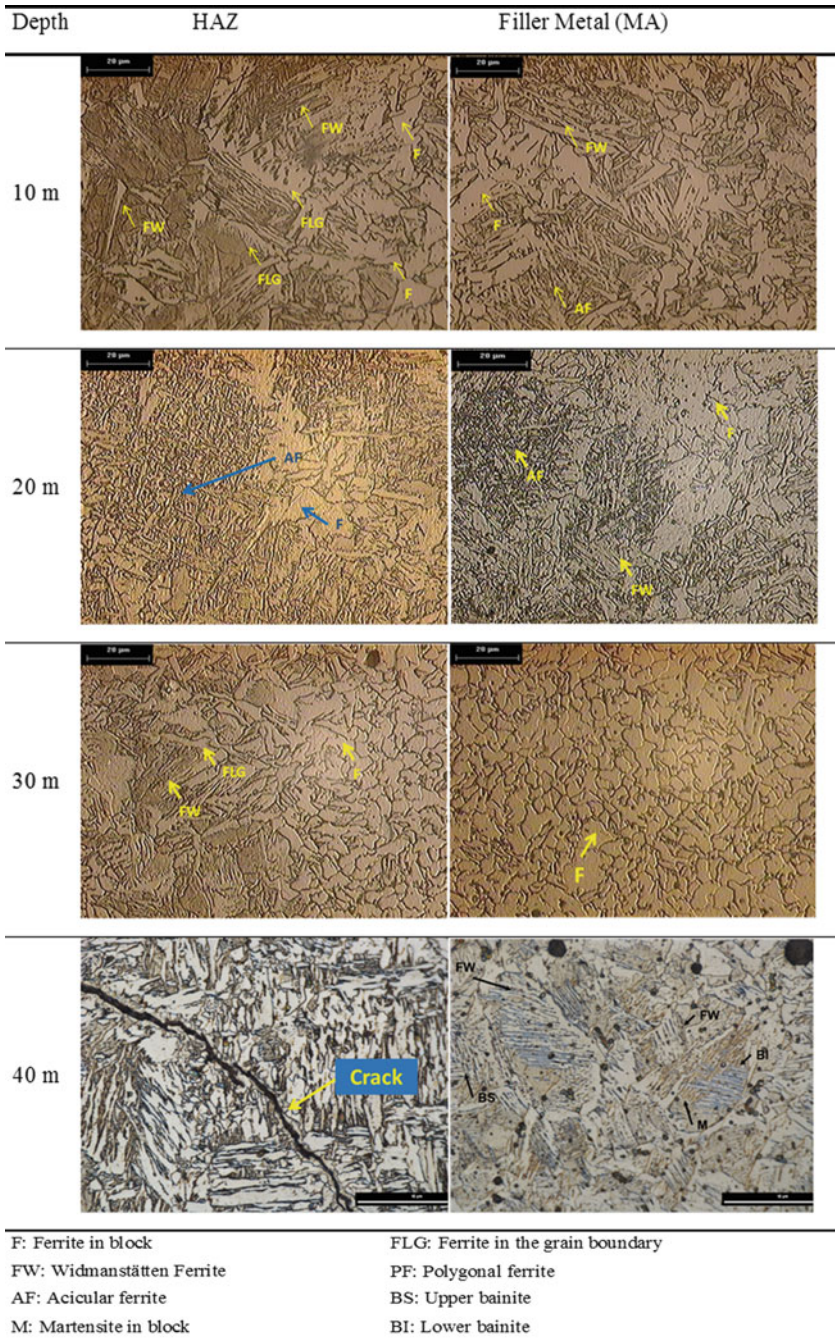


Fig. 3.5 Representative microstructures of weld seams at depths of 10, 20, 30, and 40 m

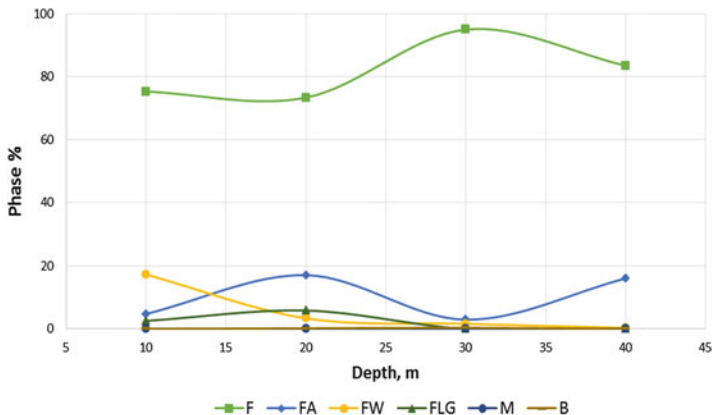


Fig. 3.6 Microstructure-depth ratio presented in the wet filler metal welding

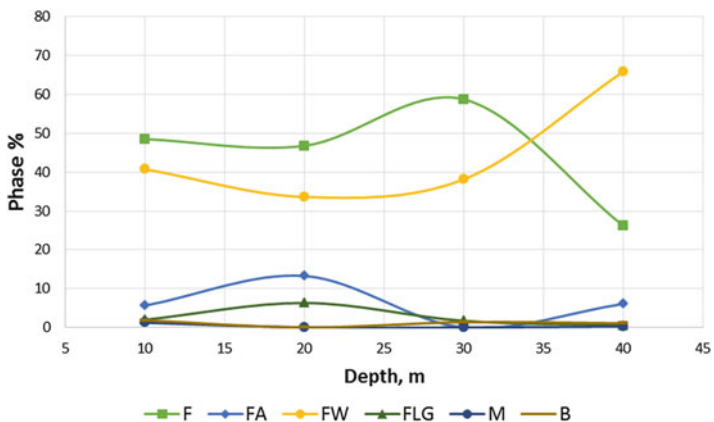


Fig. 3.7 Microstructure-depth ratio presented in the HAZ in wet welding

Table 3.3 presents a summary of the results of stress tests and microstructure, naming specimens as M1 to the depth of 10 m (33 ft), the same with the M2 to 20 m (66 ft), etc. It is shown that depth promotes a decreasing tensile strength, which is consistent with results reported by Rowe et al. [3]. This behavior regards that, as the depth increases, the porosity percentage is increasing as reported elsewhere [4]. This behavior is very noticeable in the specimens welded at 30 m and 40 m depth.

This phenomenon may be associated with the dissociation of water into H and O and the formation of CO(g) and CO<sub>2</sub>(g) that become trapped in the weld bead due to the cooling rate of the weld; In addition, the pore size increases as the depth increases [5, 12]. The reduction in mechanical properties with increasing depth is the microstructure-depth ratio obtained from the results of quantification of phases: as the depth decreases, ferrite block content and FA and the contents of FLG, FW, martensite, and bainite (the latter are found in percentages smaller than

**Table 3.3** Results of tension test and microstructure of the test coupons welded with the process MMAW to 10, 20, 30, and 40 m

Test	Classification, AWS	Depth, m (ft)	Microstructure HAZ	Tensile (MPa)
M1	E7014	10 (33)	F+FW	488
M2	E7014	20 (66)	F+FW	498
M3	E7014	30 (98)	F+FW	494
M4	E7014	40 (131)	FW	486

1 %) increase which promotes hydrogen embrittlement which explains the presence of microcracks in the sample welded at 40 m depth, as noted by Dias-da-Silva et al. [12]. The cooling rate is a major factor in the formation of microstructures hard and brittle [4, 6, 7, 13, 14]. Although an improvement was observed in stress tests at 20 m, this behavior was not expected based on those reported in the literature [8, 9]. Results suggest that due to the microstructure variation present, high contents of ferrite block up to 73 % in the weld metal and 48 % in the HAZ and 17 % of FA in the HAZ and 13 % filler metal are showed. The two main trends to decreases the mechanical properties are the porosity ratio and the phases ratio during solidification, obtaining the highest tensile stress at 20 m of depth.

### 3.4 Conclusions

Based on the experiments it is concluded:

- In the process of repairing structural components used in welding excellence in marine environment is the MMAW process due to its efficiency in time and cost.
- There is a tendency of depth-owned mechanical wet welding; with increasing depth, the tensile strength decreases, keeping properties of filler metal constant.
- It was noted that in the microstructure-depth ratio structural steels with EC < 0.37 %, the HAZ shows an increase of content of FW as the depth increases. While in the ferrite content and block FLM, no significant variation in the presence of martensite and bainite block percentage < 1 % was observed. The matrix in both, the weld metal and the HAZ, is the ferrite block.
- In order to decreases porosity and detrimental phases, welding must be performed at less depth. However, the size of the phases is lower by increasing the depth which can promote the properties in the intermediate conditions that are higher, as it was presented in the sample at 20 m.
- The addition of alloying elements such as boron and titanium and adequate control of the oxygen content and manganese acicular ferrite formation which impact on increasing the toughness of the weld is promoted.



## References

1. Verma K, Garg HK (2012) Underwater welding-recent trends and future scope. *Int J Emerg Technol* 3:115–1120
2. Joshi AM (2012) Underwater welding, vol 2. Indian Institute of Technology, Mumbai, pp 1–5
3. Pessoa ECP, Bracarense AQ, Zica EM, Liu S, Perez-Guerrero F (2006) Porosity variation along multipass underwater wet welds and its influence on mechanical properties. *J Mater Process Technol* 179:239–243
4. Johnson RL (1997) The effect of water temperature on underbead cracking of underwater wet weldments. Naval Postgraduate School, Monterey
5. Hernández-Gutiérrez P (2011) Comportamiento microestructural de un acero API-5L-X52 soldados por el proceso MMAW en ambientes marinos. COMIMSA, Saltillo
6. Ballesteros-Hinojosa, A (2012) Analisis de la generacion de esfuerzos residuales en uniones soldadas en el acero API 5L-X65 aplicadas a diferentes profundidades en ambientes submarinos por el proceso de soldadura húmeda. COMIMSA, Saltillo
7. Quintana-Puchol R, Perdomo-Gonzalez L, Bracarense AQ, Pessoa ECP (2009) Thermodynamic considerations between pores formation and hydrostatic pressure during underwater wet welding. *Soldagem Insp* 14:161–169
8. Perez-Guerrero F, Liu S (2007) The mechanism of porosity formation in underwater wet welds. *Defect Anal Mitigation* 9:215–218
9. PEMEX. NRF-175-PEMEX-2013 (2013) Acero estructural para plataformas marinas, México (2013)
10. AWS (2004) Specification for carbon steel electrodes for shielded metal arc welding ANSI/AWS A5.1. American Welding Society, Miami
11. American Weilding Society (2010) Underwater welding code AWS D3.6M, 5th edn. American Welding Society, Miami
12. Dias-da-Silva WC, Ribeiro LF, Bracarense AQ, Pessoa ECP (2012) Effect of the hydrostatic pressure in the diffusible. In: *Materials Technology; Polar and Arctic Sciences and Technology; Petroleum Technology Symposium*, vol 6, pp 1–8
13. Babu SS (2004) The mechanism of acicular ferrite in weld deposits. *Curr Opin Solid State Mater* 8:267–278
14. ASTM A36 (1998) Standard specification for carbon structural steel. ASTM, United States